

Thermal Simulation of the Continuous Pulse Discharge for Electro-spark Deposition Diamond Wire Saw

Chengyun Li

Shandong University

Peiqi Ge (✉ pqge@sdu.edu.cn)

Shandong University

Wenbo Bi

Shandong University

Research Article

Keywords: Diamond wire saw, ESD, Continuous pulse discharge, Thermal analysis

Posted Date: June 9th, 2021

DOI: <https://doi.org/10.21203/rs.3.rs-585874/v1>

License:  This work is licensed under a Creative Commons Attribution 4.0 International License.

[Read Full License](#)

Version of Record: A version of this preprint was published at The International Journal of Advanced Manufacturing Technology on January 4th, 2022. See the published version at <https://doi.org/10.1007/s00170-021-08444-x>.

1 **Thermal simulation of the continuous pulse discharge for** 2 **electro-spark deposition diamond wire saw**

3 Chengyun Li¹, Peiqi Ge^{1,2*}, Wenbo Bi¹

4 *1. School of Mechanical Engineering, Shandong University, Jinan 250061, China*

5 *2. Key Laboratory of High-Efficiency and Clean Mechanical Manufacture at*
6 *Shandong University, Ministry of Education, Jinan 250061, China*

7 *Corresponding author. Tel. /Fax.: +86 531 88399277. Email: pqge@sdu.edu.cn

8 Email address: cyli@mail.sdu.edu.cn (Chengyun Li), pqge@sdu.edu.cn (Peiqi Ge),
9 biwenbo@sdu.edu.cn (Wenbo Bi).

10 11 **Abstract**

12 Due to their excellent physical and mechanical properties, third-generation super-hard
13 semiconductor materials (such as SiC, GaN) are widely used in the field of
14 microelectronics. However, due to its ultra-high hardness, the machining is very
15 difficult, which has become the bottleneck of its development. The electro-spark
16 deposition (ESD) process can deposit electrode materials on the substrate under the
17 condition of low heat input to achieve metallurgical bonding between metal materials.
18 And it can improve the wear resistance, corrosion resistance, and repair the size of the
19 workpiece. It has been widely used in the field of surface modification engineering. It
20 can effectively improve the bonding strength of the abrasive grains, and the sawing
21 ability of the wire saw to make the consolidated diamond wire saw by the ESD
22 process. Due to its thin matrix and poor thermal properties, the saw wire is easy to
23 burning or even breaking in the manufacturing process. At present, the selection of
24 pulse interval time in the ESD process is generally determined by the duty factor.
25 However, the pulse interval time selected according to duty factor is difficult to meet
26 the heat dissipation requirements of electro-spark deposition diamond wire saw
27 (ESDDWS). In this paper, two kinds of motion modes of ESDDWS manufacturing
28 are put forward, according to the manufacturing characteristics of ESDDWS. The
29 boundary conditions of the continuous pulse discharge of ESDDWS are established.
30 The thermal simulations of continuous pulse discharge of ESDDWS under two
31 motion modes are analyzed. According to the simulation results, the basis of the value
32 of pulse interval in the ESDDWS process is put forward. The effect of pulse interval
33 time on the mechanical performance of the wire saw is analyzed experimentally. The
34 results show that the discharge interval time selected base on the simulation results

35 can ensure the continuous production of the ESDDWS.

36 **Keywords:** Diamond wire saw, ESD, Continuous pulse discharge, Thermal analysis

37 **Nomenclature**

c	Specific heat capacity
h	Convection heat coefficient
I	Discharge current
k	Thermal conductivity
m	Number of discharge
q_0	Maximum heat flux
R	The radius of the plasma channel
R_j	The radius of the saw wire
r	Coordinates of cylindrical work domain
T	Temperature
T_0	Environment temperature
t	Time
t_{on}	Pulse duration time
t_{off}	Pulse interval time
z	Coordinates of cylindrical work domain
β	The angle between the incident direction of the heat flow and the normal direction at a point on the core wire surface
θ	Coordinates of cylindrical work domain
ρ	Density

38 **1 Introduction**

39 The third-generation semiconductor materials (such as SiC and GaN) have the
40 characteristics of a high breakdown field, great charge carrier saturation, and elevated
41 dissociation temperatures. It can meet the new requirements of modern electronic
42 technology for high temperature, high voltage, high frequency, high power, and
43 radiation resistance [1, 2]. Therefore they have a broad application prospect in the
44 field of microelectronics [3, 4]. From the crystal bar to wafers, crystal machining
45 mainly includes slicing, grinding, and polishing. Slicing is the first machining
46 procedure that directly affects the subsequent processes [5, 6]. However, due to its
47 ultra-high hardness, the machining is very difficult, which has become the bottleneck
48 of its development [7].

49 Fixed diamond wire saw has become the main tool for slicing hard and brittle
50 materials [8, 9]. At present, fixed diamond wire saw mainly includes resin diamond

51 wire saw and electroplated diamond wire saw. The diamonds are attached to a core
52 wire by resin or electroplated [10]. Diamonds are less strongly bonded and have
53 shorter service life due to easy drop-off and wear of the abrasive layer [11]. Slicing
54 the super hard crystal is very difficult and inefficient [12]. In order to improve the
55 slicing efficiency, it is necessary to improve the holding strength and wear resistance
56 of the DWS.

57 ESD is a deposition process in which the electrode material is deposited on the metal
58 substrate by applying a short duration and high current pulse between cathode and
59 anode [13, 14]. It has become the new surface treatment technology that improves
60 the wear resistance and corrosion resistance of workpieces. Many research results
61 show that the substrate can be kept close to room temperature with less heat input, and
62 the mechanical properties of the substrate can be maintained [15]. Obviously, this is
63 only for large-size workpieces. Adam et al. [16] found that the range of the
64 heat-affected zone was 10 to 20 μm . At present, the diameter of the DWS matrix is 50
65 to 450 μm , and there is a decreasing trend. Therefore, the thermal effect on the saw
66 wire can not be ignored during the ESDDWS process. It is necessary to research the
67 temperature field in the continuous pulse discharge of the ESDDWS process.

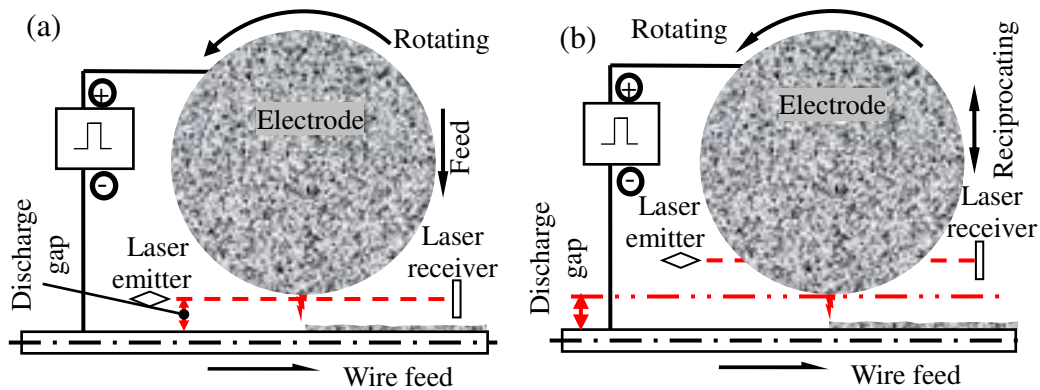
68 The discharge interval is an important factor in the ESD process. It influences the
69 discharge state and heat diffusion [17]. However, there are little researches on the
70 selection of pulse interval time in the ESD process. And it is determined mainly by the
71 duty factor. Jain et al. [18] considered that the duty factor of ESD could be between
72 40% and 86%. He has studied the influence of the duty factor on the height and width
73 of the deposition layer through experiments. The results show that the height and
74 width of the deposition layer increase with the increase of the duty factor. Mohri et al.
75 [19] considered that the duty factor of the ESD should be less than 6%. Furutani et al.
76 [20–22] fabricated wire saw in kerosene medium by ESD, and the duty factor was
77 3%. However, it was found that the wire is broken frequently when the current
78 exceeds a certain range during the fabrication process. Obviously, the ESDDWS
79 process is different from the surface treatment for the large-size workpiece. Because
80 the size of the workpiece is hundreds or even thousands of times larger than the size
81 of the discharge channel, the local temperature of deposition point has little effect on
82 the overall temperature of the substrate, which can make the workpiece almost keep at
83 room temperature. Due to its thin diameter and poor heat dissipation performance, the
84 saw wire is sensitive to the temperature increasing during the ESDDWS process.

85 In this work, two kinds of motion modes of ESDDWS manufacturing were put

86 forward, according to the manufacturing characteristics of ESDDWS. The boundary
 87 conditions of continuous pulse discharge of ESDDWS were established. The thermal
 88 simulations of continuous pulse discharge of ESDDWS under two motion modes
 89 were analyzed. According to the simulation results, the basis of determining the pulse
 90 interval time in the ESDDWS process was put forward. The effect of pulse interval
 91 time on the mechanical performance of the wire saw is analyzed experimentally. The
 92 results show that selected the discharge interval time base on the simulation results
 93 can ensure the continuous production of ESDDWS.

94 **2 The principle of fabrication of ESDDWS**

95 The principle of fabrication of ESDDWS has been studied [23]. It is not difficult to
 96 find the particularities of the ESDDWS process. Generally, the surface modification
 97 technology requires a certain thickness of the deposited layer to meet the specific
 98 performance requirements, so it needs to be repeated deposition in a certain area.
 99 However, the DWS only needs one abrasive layer. Under proper parameters, the
 100 requirement of consolidated diamond grains can be satisfied after several pulses or
 101 even one pulse of deposition in the ESDDWS process.



102
 103 Fig.1 Move model of electrode and wire

104 According to the characteristics of the ESDDWS process, the movement modes of
 105 electrode and wire can be divided into two styles (as shown in Fig.1). (1) During the
 106 manufacturing process, the electrode and matrix maintain a fixed gap. The electrodes
 107 rotate uniformly and the matrix feeds uniformly. Meanwhile, the circumferential
 108 velocity of the electrode is equal to the velocity of the core wire. The feed of the
 109 electrode is controlled by a laser limiter. (2) In the manufacturing process, the wire
 110 remains stationary during the reciprocating movement of the electrode. When the
 111 electrode returns to its original position, the wire moves forward for a distance and the
 112 electrodes rotate for an angle. The feed of the electrode is automatically adjusted by
 113 reciprocating motion.

114 In order to simplify the calculation, there are some assumptions made as follows.
 115 (1) In the manufacturing process, the arrangement of the core wire and electrodes
 116 makes the electrode column face to the surface of the matrix;
 117 (2) In the process of manufacturing, the discharge is single-channel discharge and
 118 normal spark discharge;
 119 (3) The discharge points are at the minimum gap between the core wire and the
 120 electrode;
 121 (4) The shape of both electrode and core wire is ideal. It is ignoring the change of
 122 electrode material consumption and wire surface material accumulation.

123 3 Thermal simulation of ESDDWS

124 3.1 Governing equations of heat conduction

125 For the transient, non-linear thermal analysis of the ESD process, the governing
 126 Fourier heat conduction equation [24, 25] is given by Eq. (1):

$$c\rho \frac{\partial T}{\partial t} = k \left(\frac{\partial^2 T}{\partial r^2} + \frac{1}{r} \frac{\partial T}{\partial r} + \frac{\partial^2 T}{\partial z^2} \right) \quad (1)$$

127 Where r and z are the coordinates of the cylindrical work domain; T is temperature; ρ ,
 128 c , k , and t are mass density, specific heat capacity, thermal conductivity, and time,
 129 respectively.

130 3.2 Boundary conditions

131 The single discharge surface heat source of the core wire [23] can be given as Eq.
 132 (2):

$$q(\theta, r) = q_0 \exp\left(-4.5 \frac{r^2}{(a^2 \cos^2 \theta + b^2 \sin^2 \theta)}\right) \cos \beta; \quad \begin{cases} R(t) < R_j, a = b = R(t) \\ R(t) > R_j, a = R(t), b = R_j \end{cases} \quad (2)$$

133 Where θ is the coordinates of the cylindrical work domain; β is the angle between the
 134 incident direction of the heat flow and the normal direction at a point on the core wire

135 surface, $\beta = \arcsin \frac{r \cos \theta}{R_j}$.

136 Eq. (2) only consider the heat flux on pulse duration time. The continuous pulse
 137 discharge boundary conditions of the core wire can be given as Eq. (3)

$$k \frac{\partial T}{\partial \mathbf{n}} = \begin{cases} q(\varphi, r); & m(T_{on} + T_{off}) < t \leq m(T_{on} + T_{off}) + T_{on}, 0 < r \leq R \\ h(T - T_0); & m(T_{on} + T_{off}) < t \leq m(T_{on} + T_{off}) + T_{on}, r > R \\ h(T - T_0); & T_{on} + m(T_{on} + T_{off}) < t \leq (m+1)(T_{on} + T_{off}) \end{cases} \quad (3)$$

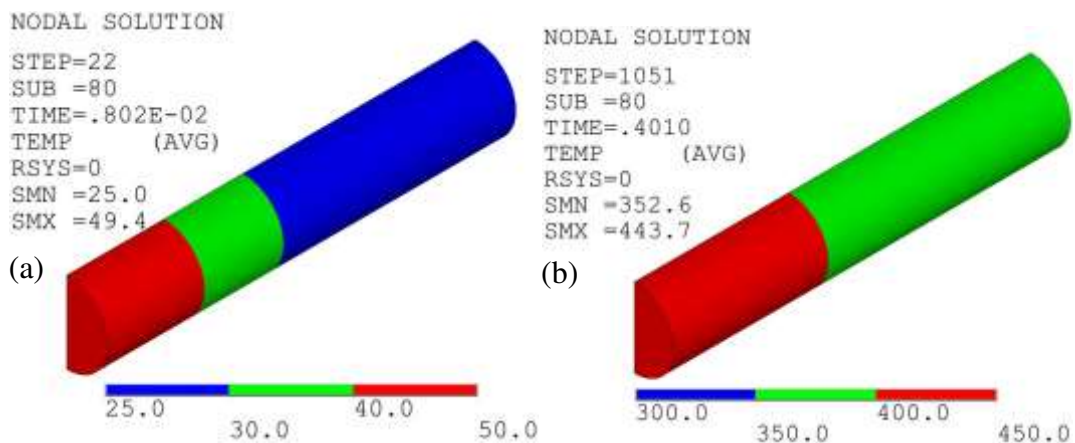
138 Where h is the convection heat transfer coefficient; k is the thermal conductivity; R is
 139 the radius of the plasma channel; m is the number of discharges. Initial temperatures

140 of the core wire are assumed to be uniform at environment temperature, $T_0 = 25^\circ\text{C}$.

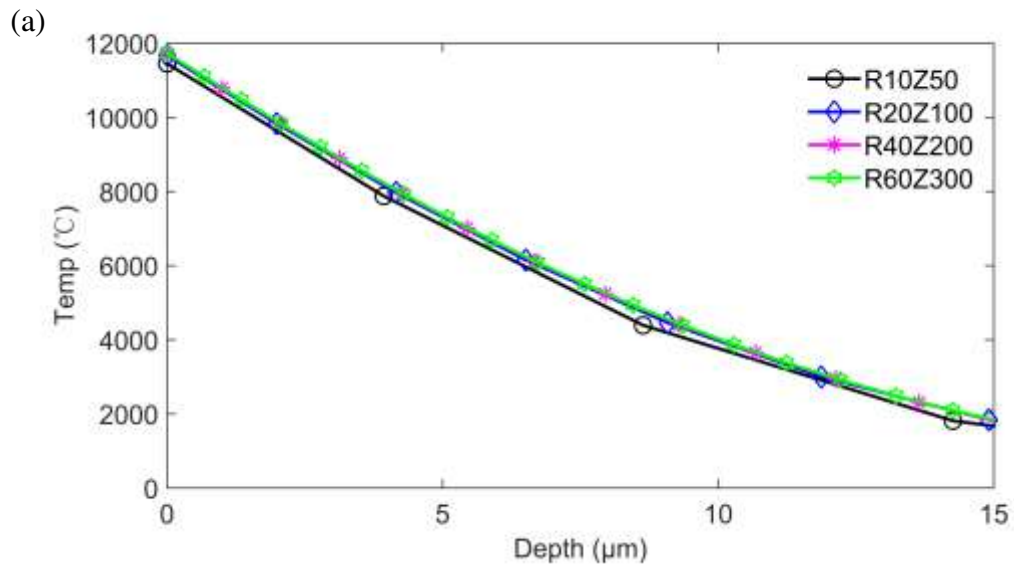
141 3.3 Meshing

142 Generally, the thermal analysis model of ANSYS is a closed model. In single pulse
143 analysis, the heat-affected zone of discharge point is smaller because of the short
144 action time and less heat input. Limited models can already meet the requirements of
145 simulation (shown in Fig.2(a)). However, Due to the long action time and the high
146 total heat input, the limited model can not meet the requirements in the continuous
147 pulse discharge deposition process, which increases the saw wire temperature (shown
148 in Fig.2(b)). Based on the element independence analysis (shown in Fig.3), the
149 element size is determined to be $3 \times 2 \times 2 \mu\text{m}$. Although, increasing the number of
150 elements can alleviate the problem of temperature accumulate without changing the
151 element size. However, increasing the number of elements will result in the
152 calculation time substantial increase.

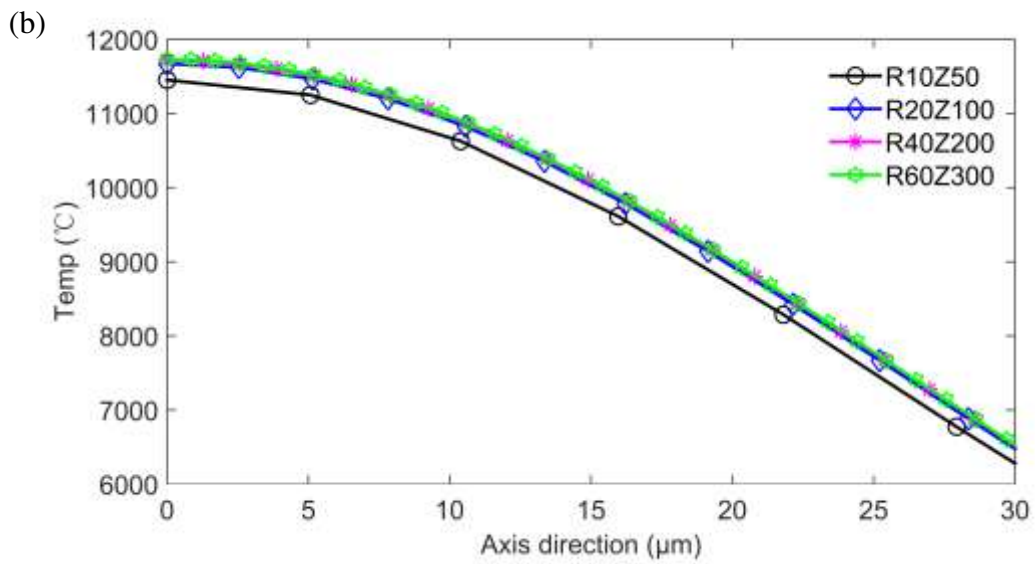
153 Based on the physical model of the ESDDWS, we can see that the saw wire is slender,
154 and the heat can be transferred infinitely in the axial direction of the core wire during
155 the deposition process. That is, the boundary of the wire saw on the axis is open. In
156 ANSYS software, the far-field element can solve the problem, which is the infinite
157 boundary of heat transfer. For 3D transient thermal simulation, the infin111 unit
158 should be selected. It should be noted that the far-field elements have only one layer
159 and require an infinite boundary load on the outside. According to the symmetry of
160 the saw wire, the meshing model of continuous pulse discharge thermal simulations of
161 ESDDWS is shown in Fig.4.



163 Fig.2 Temperature field of ESDDWS: (a) Single period temperature field; (b)
164 Continuous pulse discharge temperature field without infinite element



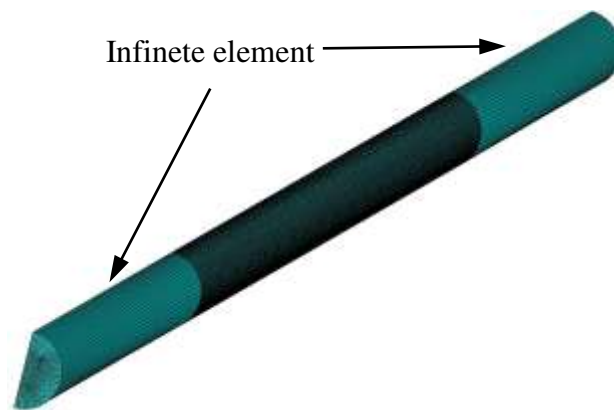
165



166

167

Fig.3 The element independence analysis: (a) depth direction; (b) axis direction



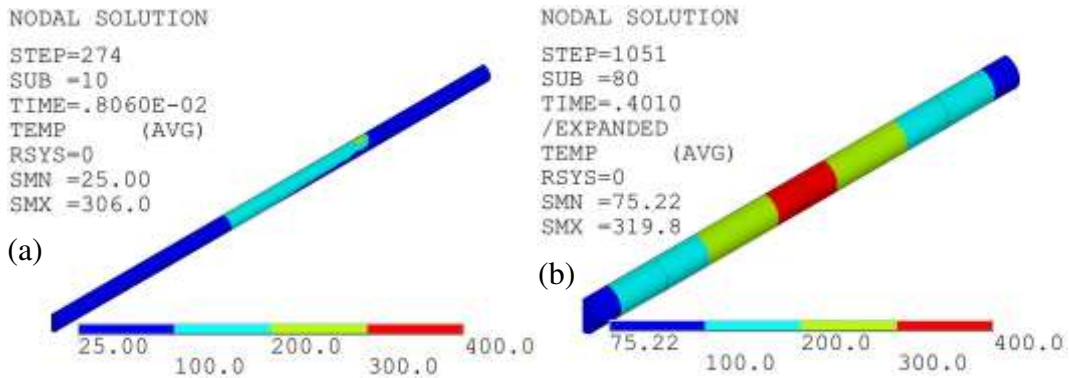
168

169

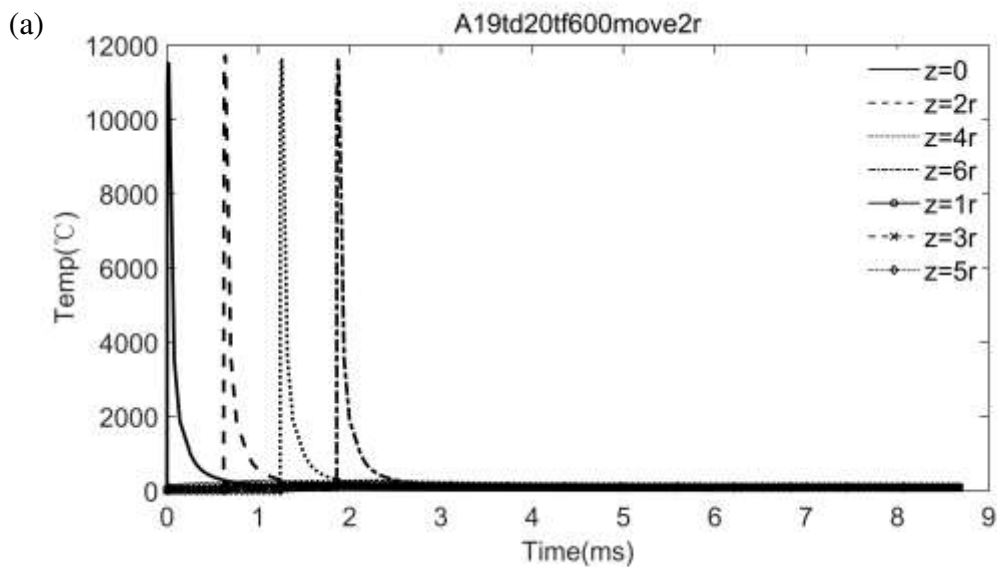
Fig.4 Meshing model of saw wire

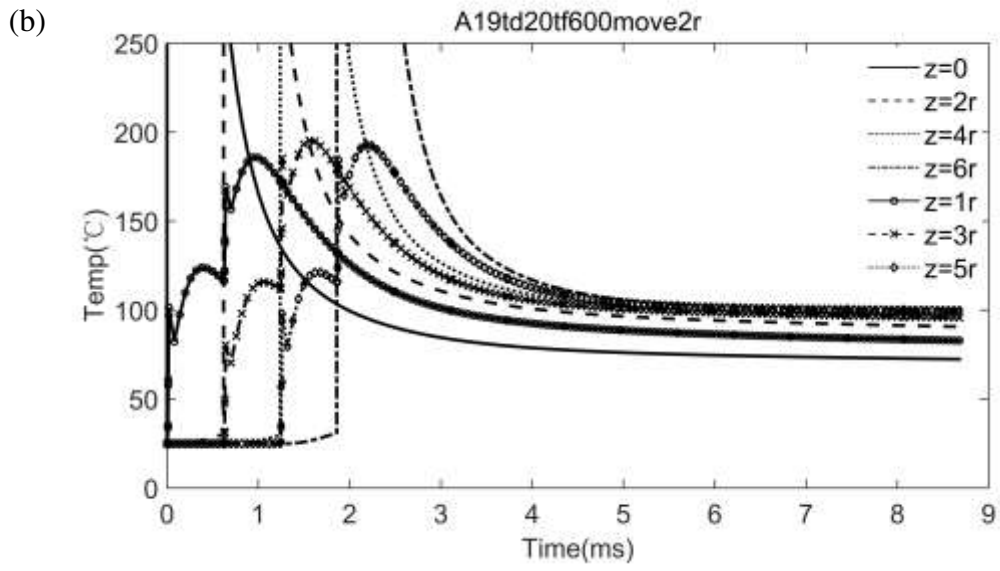
170 **4 Simulation results and discussion**

171 In this work, the diamond abrasive used W40 Ti coated diamond. The selection of
 172 discharge parameters based on the condition, the melting volume of electrode material
 173 is the volume of diamond girt's 5, 10, and 15 times. According to the prediction range
 174 of the process parameters [23], the discharge parameters determined as follows. The
 175 current is 19A, and the pulse duration time is 12 μ s, 20 μ s, and 30 μ s. The thermal
 176 simulations of continuous pulse discharge of ESDDWS under two motion modes are
 177 analyzed. Under motion mode 1, when the current is 19A, the pulse width is 20 μ s, the
 178 pulse interval is 600 μ s, and the moving speed is one discharge channel diameter per
 179 period. The temperature field of continuous pulse discharge deposition is shown in
 180 Fig.5(a). Under motion mode 2, when the current is 19A, the pulse width is 20 μ s, and
 181 the pulse interval time is 8ms. The temperature field of continuous pulse discharge
 182 deposition is shown in Fig.5(b).

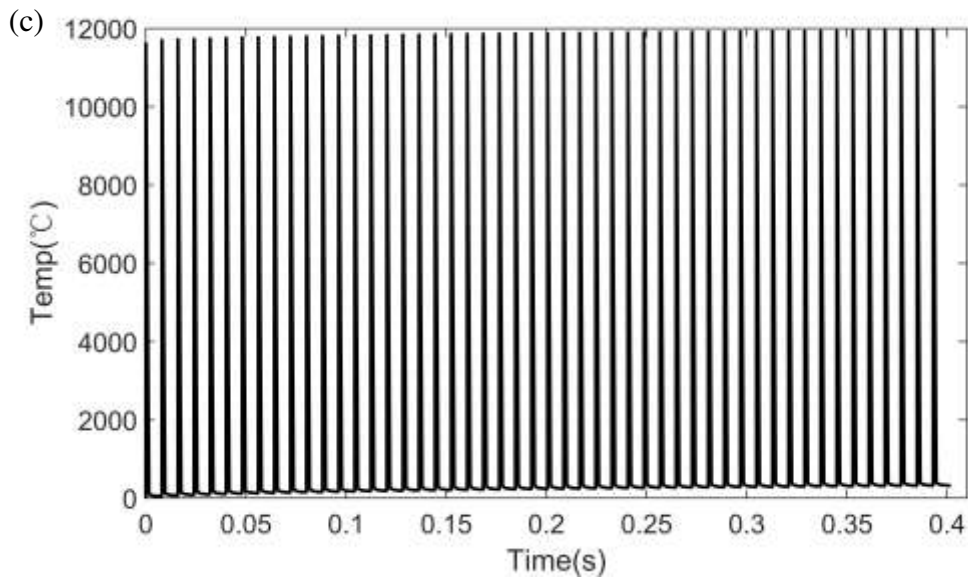


183
 184 Fig.5 Temperature field of continuous pulse discharge deposition: (a) move motion 1;
 185 (b) move motion 2

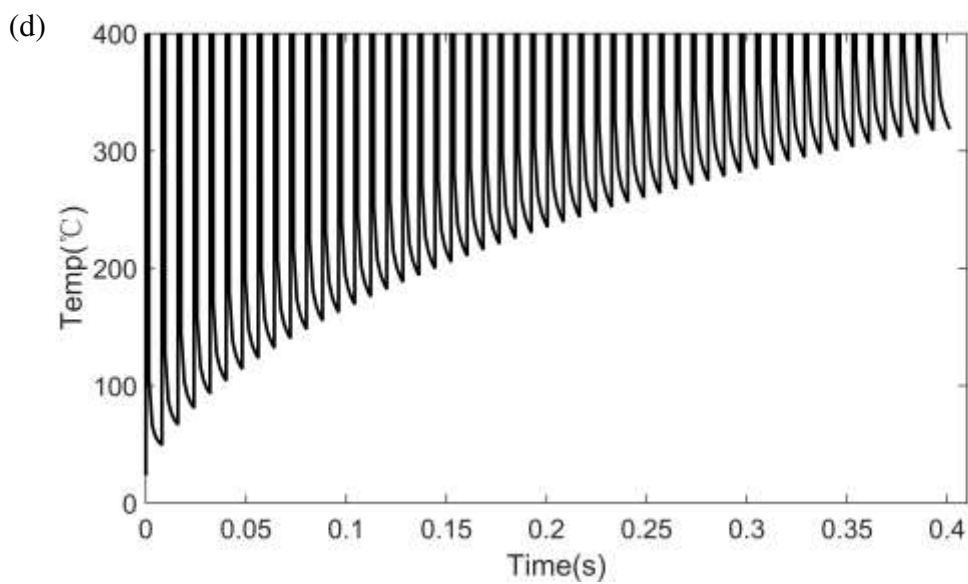




187



188



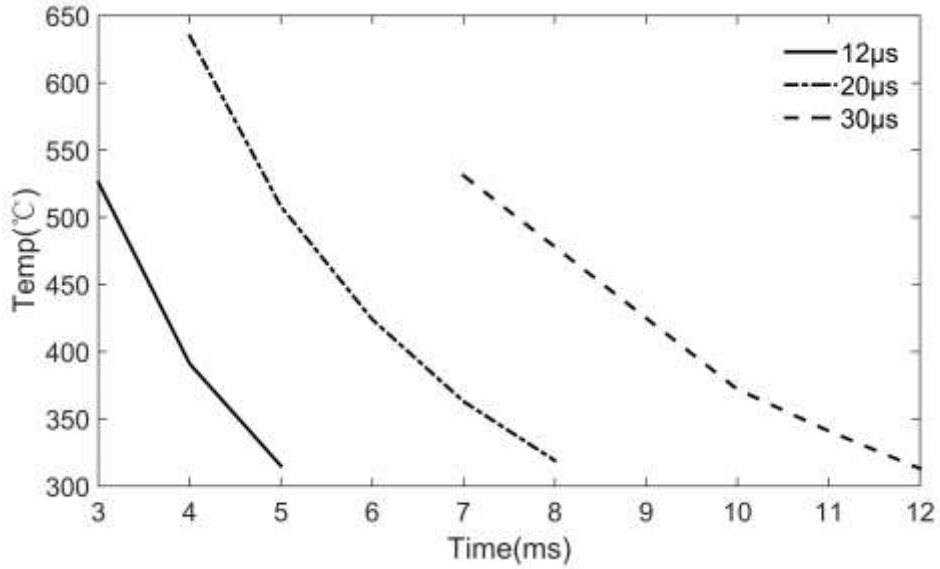
189

190 Fig.6 Temperature curve of the discharge center; (a) move model 1; (b)
191 low-temperature stages of move model 1; (c) move model 2;(d) low-temperature
192 stages of move model 2

193 From Fig.6(a) and (c), it can be seen that during a discharge period, whatever mode 1
194 or 2, the core wire's temperature rises rapidly, and then decreases rapidly. At the
195 heating stages, the heating rate can reach $6 \times 10^9 \text{C/s}$. After discharging, the cooling
196 process can be divided into two stages. At the high-temperature stages, the
197 temperature of the core wire decreases rapidly, and the cooling rate is similar to the
198 heating rate. At the low-temperature stages, the cooling rate decreases gradually.

199 By comparing the temperature curves, it can be seen that there is a big difference
200 between motion modes 1 and 2. In motion mode 1, there is no mutation in the
201 temperature-time curves of adjacent discharge centers such as $z=0$, $z=2r$, $z=4r$, and
202 $z=6r$. It indicates that the temperature of the next discharge center is not affected by
203 the previous discharge. There are two abrupt mutations in the temperature curve of the
204 edge point of the discharge channel in a period. And there are four mutations in total
205 such as $z=r$, $z=3r$, and $z=5r$. The first mutation is caused by the heat source and then
206 decreases with the end of discharge. The second mutation is due to the diffusion of a
207 large amount of heat from the discharge center. It indicates that the adjacent
208 discharges have an impact on the edge point of the discharge channel. The effect of
209 temperature superposition can be ignored when the distance between two discharge
210 points is greater than three times the discharge channel radius. Finally, the core wire
211 tends to equilibrium temperature. In motion mode 2, the discharge centers are in the
212 same position. During the increase of discharge times, the core wire's temperature
213 increases continuously due to the superposition of energy.

214 We take the final temperature at the discharge center as the dynamic equilibrium
215 temperature of the core wire. According to the ANSYS simulation results, the
216 relationship between the core wire equilibrium temperature and the pulse interval time
217 in movement model 2 has obtained, as shown in Fig.7.



218

219 Fig.7 The relationship of balance temperature of wire and pulse interval duration
 220 time(move model 2)

221 **5 Experiments**

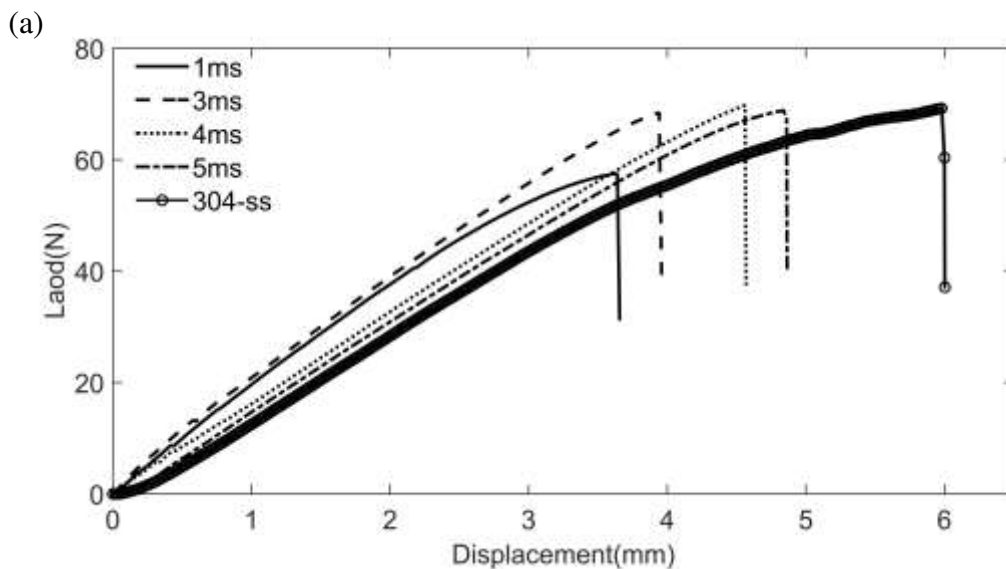
222 The manufacturing experiment is carried out on a self-made ESD machine, and the
 223 saw wire was deposited from one side. The experimental parameters are described in
 224 Table 1.

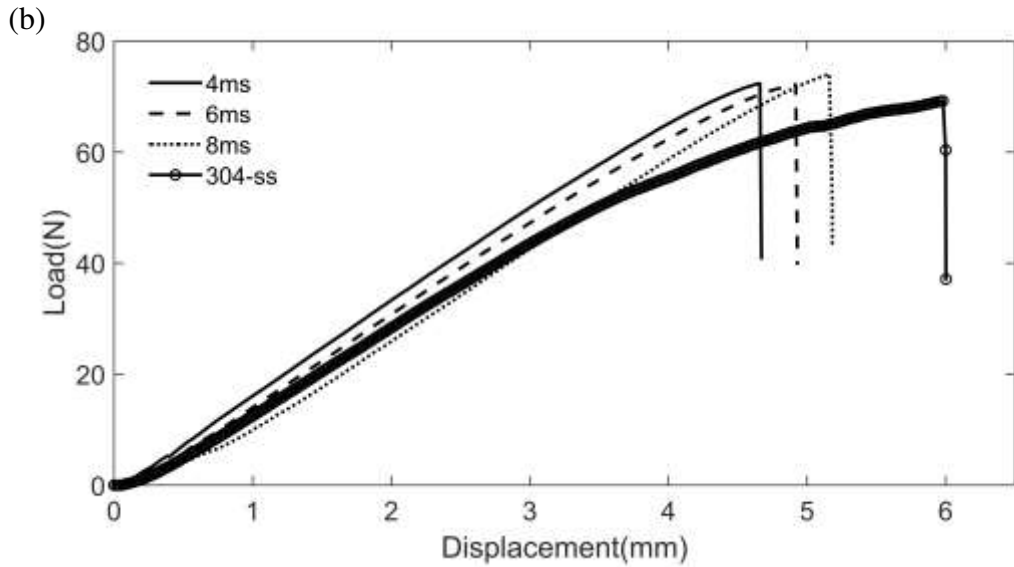
Table. 1 Experiment parameter

Parameter	Value										
Workpiece (Cathode)	304-ss(ϕ 0.2mm)										
Electrode (Anode)	Cu(10 μ m):Ni(10 μ m):Diamond=12:12:1										
Coated diamond	W40										
Current(A)	19										
Pulse duration time(μ s)	12			20			30				
Pulse interval time(ms)	1	3	4	5	4	6	8	6	8	10	
Working medium	Air										
Movement mode	2										
Discharge time(s)	0.4										

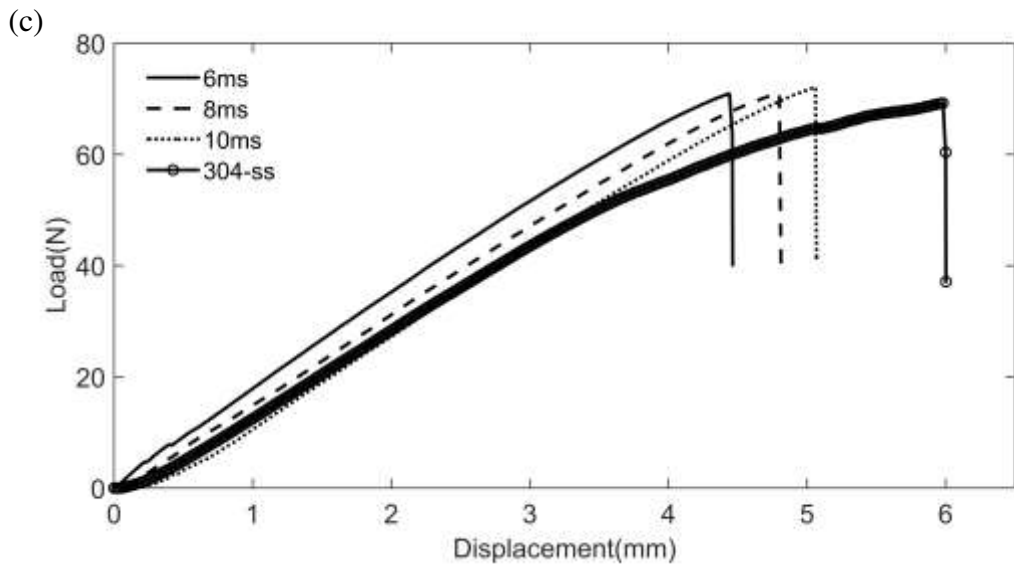
225 The mechanical properties of the 304-ss wire changed because of the microstructure's
 226 transformation. Because it is slender, the change of local structure will affect the
 227 overall performance of the core wire. Researchers have reported that the martensitic
 228 transformation of 304-ss begins at 300°C [26]. Therefore, the local equilibrium
 229 temperature of the saw wire should maintain at about 300°C during the ESDDSW
 230 process. Therefore, select the pulse interval time should base on the discharge

231 parameters. In the experiment, when the pulse duration time is $12\mu\text{s}$, the pulse interval
 232 time is set to 1ms, 3ms, 4ms, and 5ms. When the pulse duration time is $20\mu\text{s}$, the
 233 pulse interval time is set to 4ms, 6ms, and 8ms. When the pulse duration time is $30\mu\text{s}$,
 234 the pulse interval time is set to 6ms, 8ms, and 10ms. During the experiment, when the
 235 pulse duration time is $12\mu\text{s}$ and the pulse interval time is 1 ms, the saw wire is broke
 236 frequently. And the saw wire deforms obviously after deposition. Under other
 237 parameters, the saw wire does not break, and the saw wire keeps its original shape.
 238 Tensile tests have been carried out on the deposited wire saw, and the
 239 load-displacement curve is shown in Fig.8. It can be seen that: when the pulse
 240 duration time is $12\mu\text{s}$ and the pulse interval time is 1 ms, the wire breaking force is
 241 10N lower than that of the raw wire. And its ductility is also greatly reduced. Under
 242 other parameters, with the decrease of pulse interval time, the broken force of the saw
 243 wire does not decrease obviously, but its ductility also decreases gradually. It
 244 indicated that the pulse interval would first affect the plasticity of the wire saw. And
 245 when it exceeds a certain range, it would affect the tensile strength of the wire saw.
 246 Therefore, in order to maintain its mechanical performance, the balance temperature
 247 of the wire saw should be around 300°C during the ESDDWS process.





249



250

251 Fig.8 Load and displacement curve of tensile test:(a) $12\mu\text{s}$; (b) $20\mu\text{s}$; (c) $30\mu\text{s}$

252 **6 Conclusion**

253 (1) According to the process characteristics of ESDDWS, two kinds of motion modes
254 of manufacturing are put forward.

255 (2) According to the characteristics of the saw wire, a simulation model of continuous
256 pulse discharge deposition is established.

257 (3) According to the two different motion modes of electrode and core wire, the
258 thermal simulations of continuous pulse discharge of ESDDWS were analyzed.

259 (4) The simulation results show that: in movement mode 1, the temperature of
260 adjacent discharge points has the superposition effect. The effect of temperature
261 superposition can be ignored when the distance between two discharge points is

262 greater than three times the discharge channel radius. The wire saw's temperature
263 tends to balance finally. In motion mode 2, the discharge centers are in the same
264 position. During the increase of discharge times, the core wire's temperature increases
265 continuously due to the superposition of energy.

266 (5) The pulse interval would first affect the plasticity of the wire saw. And when it
267 exceeds a certain range, it would affect the tensile strength of the wire saw. In order to
268 maintain its mechanical performance, the balance temperature of the wire saw should
269 be around 300°C during the ESDDWS process.

270

271 **Acknowledgment**

272 This work is financially supported by the National Natural Science Foundation of
273 China (No.51775317); the Key Research and Development Program of Shandong
274 Province, China (No.2019JZZY020209)

275

276 **Declarations**

277 **Ethical approval**

278 Not applicable

279

280 **Consent to participate**

281 Not applicable

282

283 **Consent to publish**

284 The authors declare that this work has not been submitted elsewhere for publication,
285 in whole or in part.

286

287 **Authors contributions**

288 Chengyun Li is the executor of article writing and experiment operation.

289 Peiqi Ge contributed to the conception of the work.

290 Wenbo Bi contributed to the experiment preparation.

291

292 **Funding**

293 This work is financially supported by the National Natural Science Foundation of
294 China (No.51775317); the Key Research and Development Program of Shandong
295 Province, China (No.2019JZZY020209)

296

297 **Competing interests**

298 We declare that we have no financial and personal relationships with other people or
299 organizations that can inappropriately influence our work. We have no competing
300 financial interests.

301

302 **Code availability**

303 Not applicable.

304

305 **Data availability**

306 The data and materials supporting the results of this article are included within the
307 article.

308

309 **References**

- 310 [1] Yadlapalli R, Kotapati A, Kandipati R, Balusu S, Koritala C. (2021) Advancements
311 in energy efficient GaN power devices and power modules for electric vehicle
312 applications: a review. *Int J Energ Res*.
- 313 [2] Wellmann P. (2017) Power electronic semiconductor materials for automotive and
314 energy saving applications - SiC, GaN, Ga₂O₃, and Diamond. *Z Anorg Allg Chem*.
315 643(21), 1312-1322.
- 316 [3] Gao Y, Chen Y. (2019) Sawing stress of SiC single crystal with void defect in
317 diamond wire saw slicing. *Int J Adv Manuf Tech*. 103(1-4), 1019-1031.
- 318 [4] Garrido D, Baraia I.(2017) Review of wide bandgap materials and their impact in
319 new power devices. *IEEE (ECMSM)*. Donostia-San Sebastian, Spain.
- 320 [5] Gao Y, Chen Y, Ge P, Zhang L, Bi W. (2018) Study on the subsurface microcrack
321 damage depth in electroplated diamond wire saw slicing SiC crystal. *Ceram Int*.
322 44(18), 22927-22934.
- 323 [6] Chung C, Tsay G, Tsai M. (2014) Distribution of diamond grains in fixed abrasive
324 wire sawing process. *Int J Adv Manuf Tech*. 73(9-12), 1485-1494.
- 325 [7] Huang H, Zhang Y, Xu X. (2015) Experimental investigation on the machining
326 characteristics of single-crystal SiC sawing with the fixed diamond wire. *Int J Adv*
327 *Manuf Tech*. 81(5-8), 955-965.
- 328 [8] Kim D, Kim H, Lee S, Jeong H. (2015) Effect of initial deflection of diamond wire
329 on thickness variation of sapphire wafer in multi-wire saw. *Int J Pr Eng Man-Gt*.
330 2(2), 117-121.
- 331 [9] Huang H, Li X, Xu X. (2017) An experimental research on the force and energy
332 during the sapphire sawing using reciprocating electroplated diamond wire saw. *J*
333 *Manuf Sci E-T Asme*. 139, 121011.
- 334 [10]Tsai P, Chou Y, Yang S, Chen Y, Wu C.(2013) A comparison of wafers sawn by
335 resin bonded and electroplated diamond wire - from wafer to cell. *IEEE*
336 *(PVSC)*.Tampa, FL. 523-525.
- 337 [11]Liu T, Ge P, Gao Y, Bi W. (2017) Depth of cut for single abrasive and cutting force
338 in resin bonded diamond wire sawing. *Int J Adv Manuf Tech*. 88(5-8), 1763-1773.

- 339 [12]Kim H, Kim D, Kim C, Jeong H. (2013) Multi-wire sawing of sapphire crystals
340 with reciprocating motion of electroplated diamond wires. *CIRP Annals*. 62(1),
341 335-338.
- 342 [13]Sheldon G, Johnson R. (1985) Electro-spark deposition: A technique for producing
343 wear resistant coatings. *Wear Mater: Int. Conf. Wear Mater*. 388-396.
- 344 [14]Wang P, Pan G, Zhou Y, Qu J, Shao H. (1997) Accelerated electrospark deposition
345 and the wear behavior of coatings. *J Mater Eng Perform*. 6(6), 780-784.
- 346 [15]Chakraborty S, Kar S, Dey V, Ghosh S. (2018) The phenomenon of surface
347 modification by electro-discharge coating process: A review. *Surf Rev Lett*. 25(01),
348 1830001-1830003.
- 349 [16]Adam B, Wood W, Kadali J, Talla R, Langston T. (2017) Heat affected zone
350 formation in electrospark deposition additive manufacturing on ultrahigh strength
351 steel. *Mater Perform Charact*. 6, 375-393.
- 352 [17]Peng Z, Li Y. (2012) The deposition and removal process for micro machining
353 based on electrical discharge. *Adv Mater Res*. 472-475, 2448-2451.
- 354 [18]Jain V, Seshank S, Sidpara A, Jain H.(2013) Some aspects of micro-fabrication
355 using electro-discharge deposition process. *ASME/ISCIE (ISFA2012)*,St Louis,
356 MO. 419-424.
- 357 [19]Mohri N, Saito N, Tsunekawa Y, Kinoshita N. (1993) Metal surface modification
358 by electrical discharge machining with composite electrode. *CIRP Annals - Manuf*
359 *Techno*. 42(1), 219-222.
- 360 [20]Furutani K, Suzuki K. (2015) Experimental investigations of deposition conditions
361 for saw wire fabrication by electrical discharge machining. *Int J Adv Manuf Tech*.
362 76(9-12), 1643-1651.
- 363 [21]Furutani K, Kanai M, Mieda Y, Suzuki M. (2010) Proposal of abrasive layer
364 fabrication on thin wire by electric discharge machining. *Int J Automation Technol*.
365 4(4), 394-398.
- 366 [22]Furutani K, Suzuki K. (2009) A desktop saw wire coating machine by using
367 electrical discharge machining. *IEEE Int Conf Cont Autom*. Christchurch, New
368 Zealand. 2165-2170.

- 369 [23]Li C, Ge P, Bi W. (2021) Thermal simulation of the single discharge for
370 electro-spark deposition diamond wire saw. *Int J Adv Manuf Tech.*
- 371 [24]Wang Y, Xie B, Wang Z, Peng Z. (2011) Micro EDM deposition in air by single
372 discharge thermo simulation. *T Nonferr Metal Soc.* 21(s2), 450-455.
- 373 [25]Shahri H, Mahdavinejad R, Ashjaee M, Abdullah A. (2017) A comparative
374 investigation on temperature distribution in electric discharge machining process
375 through analytical, numerical and experimental methods. *Int J Mach Tools Manuf.*
376 114, 35-53.
- 377 [26]Alinia S, Khamedi R, Ahmadi I. (2018) An investigation into deep drawing
378 parameters on deformation induced martensitic microstructure transformation of
379 an austenitic stainless steel. *Metallogr, Microstruct, Anal.* 7(6), 724-734.
- 380

Figures

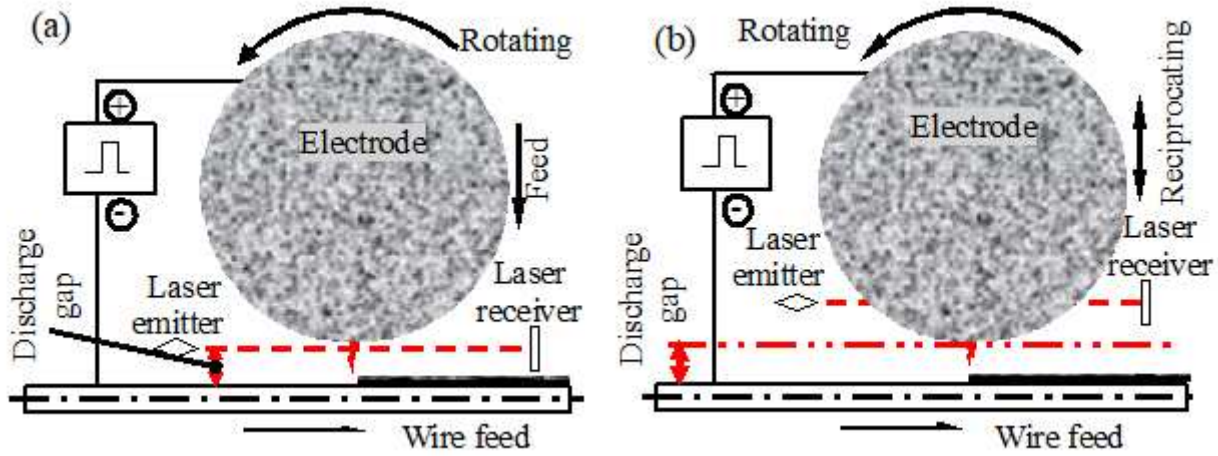
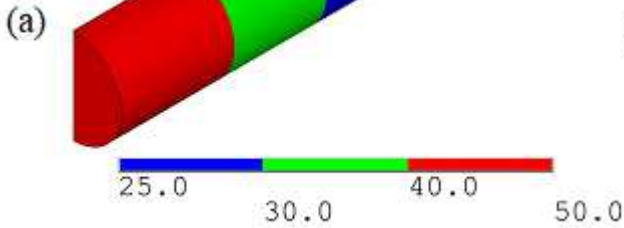


Figure 1

Move model of electrode and wire

NODAL SOLUTION

STEP=22
 SUB =80
 TIME=.802E-02
 TEMP (AVG)
 RSYS=0
 SMN =25.0
 SMX =49.4



NODAL SOLUTION

STEP=1051
 SUB =80
 TIME=.4010
 TEMP (AVG)
 RSYS=0
 SMN =352.6
 SMX =443.7

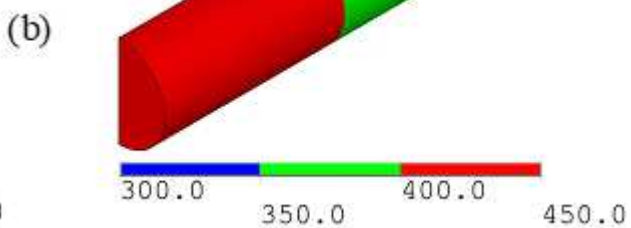


Figure 2

Temperature field of ESDDWS: (a) Single period temperature field; (b) Continuous pulse discharge temperature field without infinite element

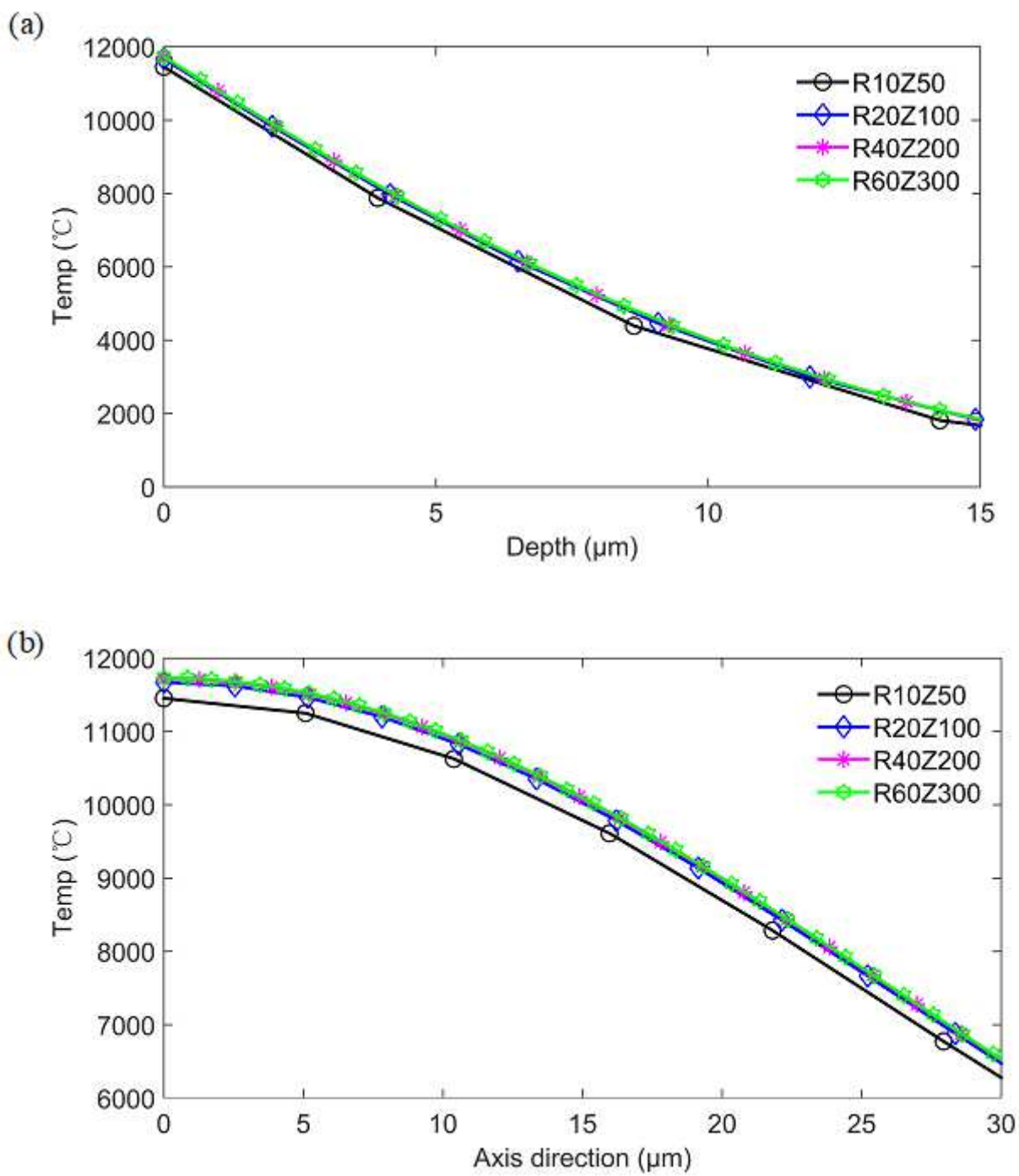


Figure 3

The element independence analysis: (a) depth direction; (b) axis direction

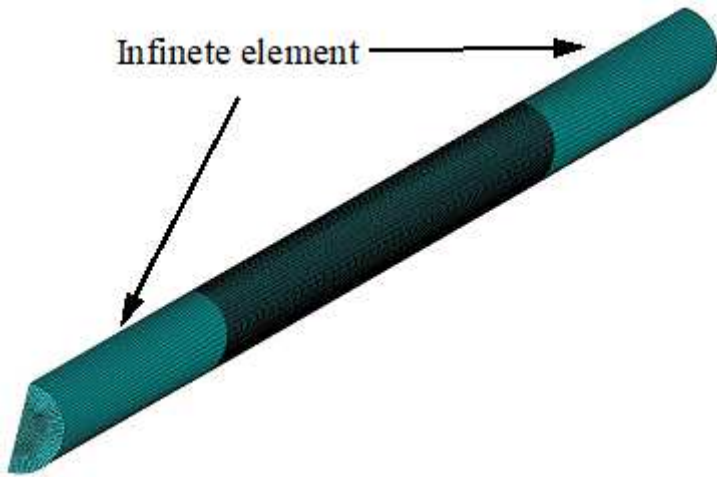


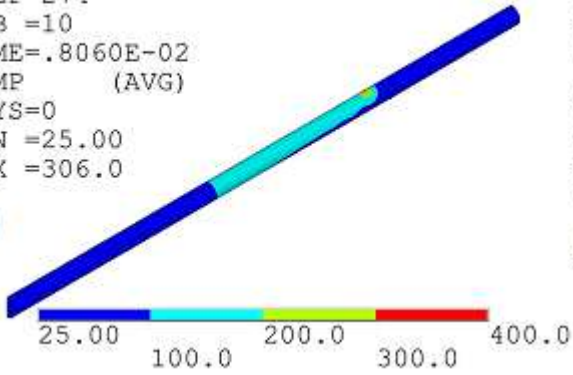
Figure 4

Meshing model of saw wire

```

NODAL SOLUTION
STEP=274
SUB =10
TIME=.8060E-02
TEMP      (AVG)
RSYS=0
SMN =25.00
SMX =306.0
  
```

(a)



```

NODAL SOLUTION
STEP=1051
SUB =80
TIME=.4010
/EXPANDED
TEMP      (AVG)
RSYS=0
SMN =75.22
SMX =319.8
  
```

(b)

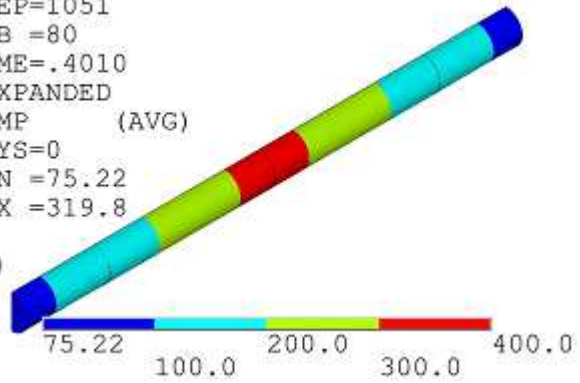


Figure 5

Temperature field of continuous pulse discharge deposition: (a) move motion 1; (b) move motion 2

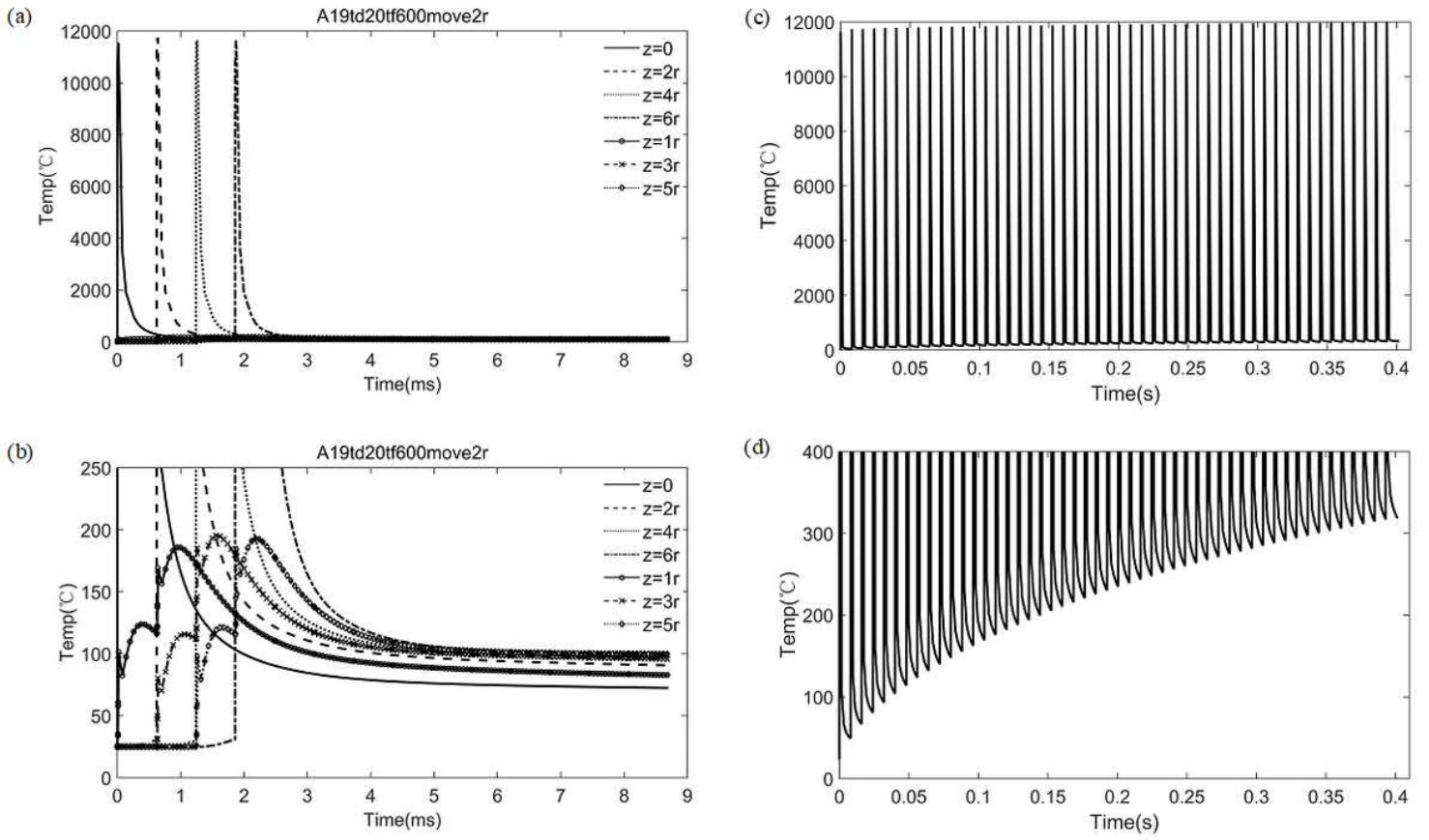


Figure 6

Temperature curve of the discharge center; (a) move model 1; (b) low-temperature stages of move model 1; (c) move model 2; (d) low-temperature stages of move model 2

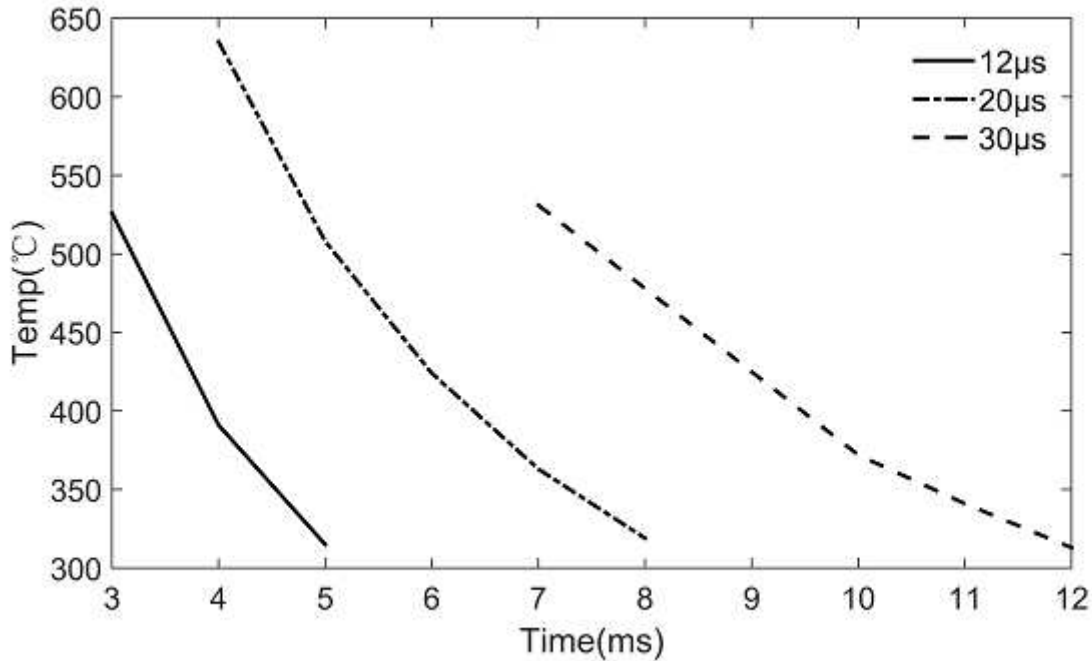


Figure 7

The relationship of balance temperature of wire and pulse interval duration time(move model 2)

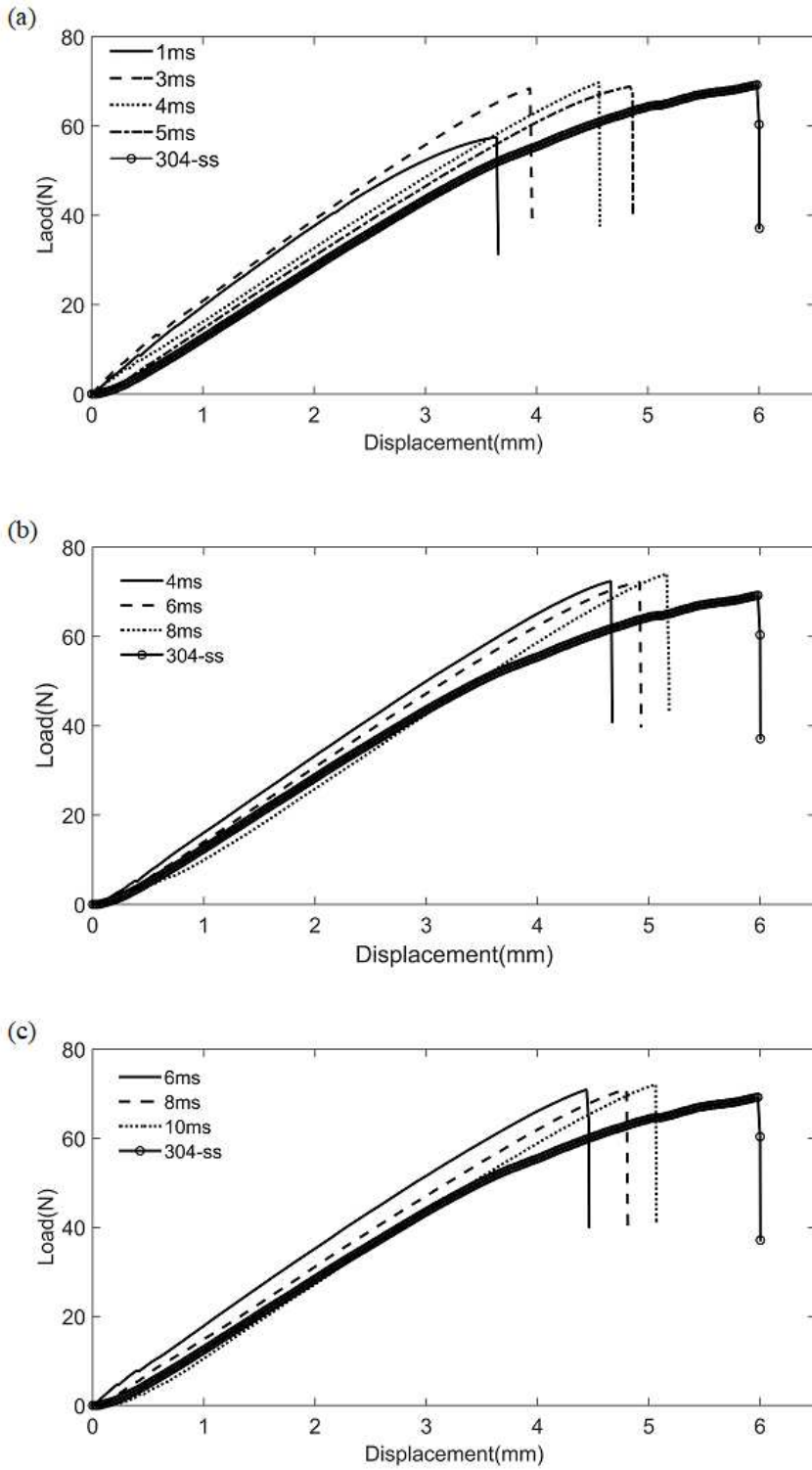


Figure 8

Load and displacement curve of tensile test:(a) 12 μ s; (b) 20 μ s; (c) 30 μ s